《Journal of Earth Science》网络首发论文

Early warning of heavy metal pollution after tailing pond failure accident

Yonggui Wang[1], Yinqun Yang[2, *], Qiang Li[1], Yaxin Zhang[1], Xiaolong Chen[3]

[1]Hubei Key Laboratory of Critical Zone Evolution, School of Geography and Information Engineering, China University of Geosciences, Wuhan 430074, China
[2]Changjiang Water Resources Protection Institute, Wuhan 430051, China
[3] Beijing Tsinghua Holdings Human Settlements Environment Institute, Beijing, 100083, China
*Corresponding author: yangyinqun@whu.edu.cn

Abstract: Heavy metal pollution is a major issue after tailing pond failure accident. It is important to predict pollution trends for limited data of pollution sources. A simple phase separation heavy metal model was built for early warning simulation of heavy metal pollution accidents. Based on this, a new simulation framework has been developed to predict the pollution trends of the downstream according to the measured data at upstream sections. By setting the upstream monitoring date as the inflow boundary condition, the changing processes of heavy metal manganese*(Mn)* with different phases in the downstream can be accurately simulated and forecasted. Results showed that the concentration of the suspended phase in the downstream was larger than that in the aqueous phase and sediment phase.With this, the early warning of pollution trends after accidents could be made a few days ahead. It indicates that the impact of sediment on heavy metal should not be ignored in the early warning of tailing pond failure accidents.

Keywords: heavy metal pollution, early warning, tailing pond failure accident, phase separation model

1 INTRODUCTION

The tailing dam accident is the 18th serious event among 39 worldwide accidents and public damages(Criss et al., 2020). It is reported that tailing pond failures are morethan 60 percent of overall tailing dam accidents(Agurto-Detzel et al., 2016). The high speed volume slurry or flood may cause heavy metal pollution and affect water security in a wide range and long duration(Jacobson and Faust, 2014). The early

warning and evaluation of heavy metal pollution are of great significance for accident emergency disposal and disaster prevention(Yuanhua et al., 2013). Therefore, it is helpful and necessary to exploit the spatial and temporal distribution of heavy metal after accident.

With the development of urbanization, industrialization and transportation, the sudden water pollution accidents occur frequently, which has attracted an enormous amount of researches. In the early stage, researches focused on the mathematical model studies for pollutant transport simulation in rivers(Ani et al., 2012; Grayman, W.M., Deninger, R.A., Males, R., 2001; Storey et al., 2011). Later on, the early warning systems (EWS) coupled with GIS and water quality models were studied and put into practice (Ding et al., 2017; Wang et al., 2018, 2015).While, most of these existing models or systems focus on soluble groundwater pollutants early warning, only a few studies focus on the pollution accidents of heavy metal, which is slightly soluble in water.Generally, the heavy metal pollution from industrial and mining wastewater spilling, heavy metal transport vehicle accident and tailings water leakage can be described by empirical formulas, regression forecast, ensemble models and mechanism models(Jähnig and Cai, 2010; Rafiei et al., 2012; Shah et al., 2013; Wang et al., 2015; Winner et al., 1980). Among which, heavy metal numerical models are widely used methods for heavy metal changing processes quantifying.In mechanism models,the physical migration processes, including heavy metal dissolution(Bambach et al., 2013; Chen et al., 2011),the adsorption-desorption on sediment (Helios Rybicka et al., 1995),and the chemical and biology transformation processes are usually considered. These physical, chemical and biology changing processes are complicated and influenced by a lot of factors, such as pH, temperature, sediment concentration and hydrodynamic conditions(Sadeghi et al., 2012), which makes numerical models accurate but need detailed data for model calibration(Djihouessi and Aina, 2018). While, as environmental accidents occur randomly in temporal and spatial spaces, such as the occurrence of tailing pond failure accidents in remote mountain areas, it is hard to obtain enough data for accident simulation in a short period. Under this emergency circumstance, numerical models are not always suitable because of requiring rich data.

For accident early warning where lack of data, it is suggested that the tendency forecasting of pollutants is helpful and more feasible(Wang et al., 2015). The main transport process of heavy metals can be simplified and divided into two parts. One is

heavy metal moving with water and soil, the other is heavy metal transforming among three phases-aqueous, suspended and sedimentary sediment(Wang et al., 2016).Previous research showed that utilizing phase separation phenomena for the heavy metal simulation is capable to describe its changing process(Chen et al., 2016).The advantage of phase separation is that parameters are fewer and easy to use. Several studies have proved that the phase separation model can model the changing trend of pollutants with limited data(Dalali and Habibi, 2015). By taking these measured data as boundary conditions, it is possible to make simulation and early warning for the downstream sensitive areas(Wang et al., 2018).

China is a country with a high-frequency of tailings dam accidents. From 2001 to 2014, over 100 tailing dam accidents happened(Yu et al., 2014). In this paper, a heavy metal simulation tool for the early warning of tailing pond failure accident was developed. With this tool, the influence and early warning of a manganese *(Mn)* tailing pond failure accident occurred in the upstream of Fujiang River induced by rainstorm has been simulated.

2 METHODS

2.1 Framework oftheheavy metal pollution accident early warning

Numerical models are widely used methods for pollutant transport simulation. According to the universal flow chart of early warning, the implementing framework of heavy metal pollution early warning after tailing pond failure accident is developed(Hasan et al., 2005), as shown in Fig. 1.
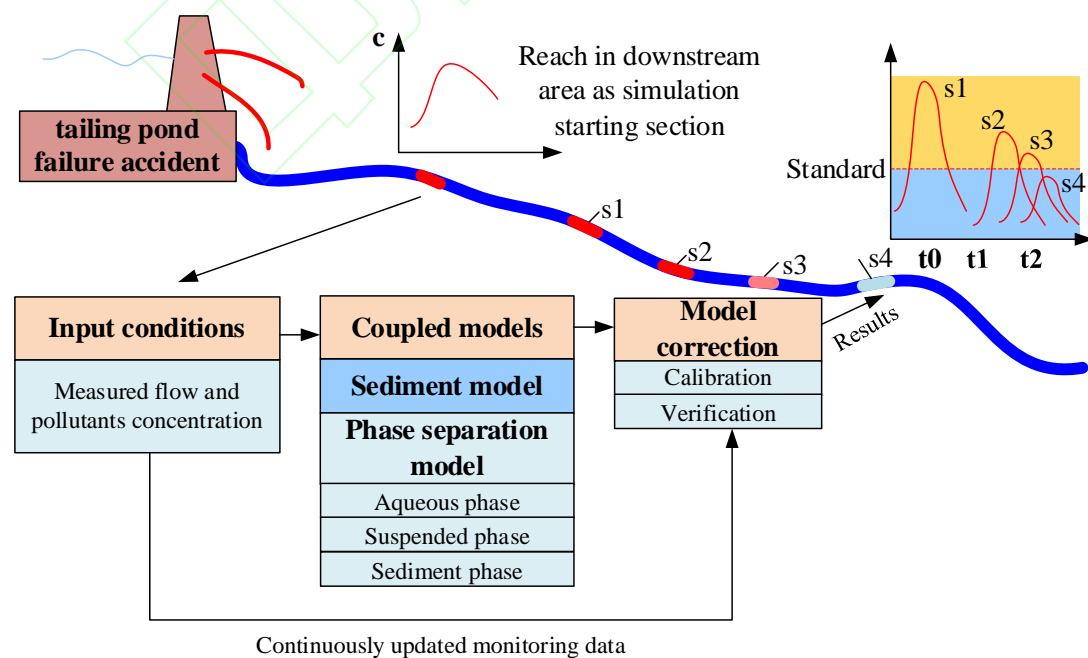
Fig. 1. The implementing framework of the heavy metal accident early warning with coupled numeric models. Where, s1,s2,s3 and s4 are simulation sections; t0, t1 and t2 are different time.

(1) Models developing

A coupled model including sediment model and phase separation model has been developed for heavy metal transport simulation, which will be described in section 2.2.

(2) Input conditions setting

For early warning, the prediction of spatial and temporal distribution in the future three days for heavy metal concentrations is helpful and indispensable (Huan et al., 2020). Input data contain initial conditions, boundary conditions and parameters. The initial conditions are determined based on measured data at the beginning of simulation time. Boundary conditions include inflow condition and lateral condition. The start reach where measured data collected in the upstream is set as inflow headwater.The lateral condition will be ignored in the early warning simulation. Two methods have been used for input data extension in the future three days. For steady flow, input conditions in the next three days can be set the same as the current day. For unsteady flow, a linear regression equation is applied according to the flow or water elevation at the previous three time points. Additionally, other time series boundary conditions, including the water level of the outflow and the value of parameterscanbe set according to the measured data.

(3) Model parameters correction

Parameters should be calibrated and corrected by measured data and simulation results. After getting the simulation results, the deterministic coefficient (R^2) and the relative error (*re*)will be used for model parameters calibration. If the $R^2$and *re* reach their goals, current parameters will be treated as determinate parameters for the next simulation. Otherwise, it is necessary to revise parameters and restart models until the $R^2$and *re* reach their goals.

2.2 Coupled model for heavy metal transport simulation

Unlike the soluble substance, the transport process of heavy metals is greatly influenced by sediments. Heavy metal in water can be simplified into transportation and transformation processes, as showed in Fig. 2.
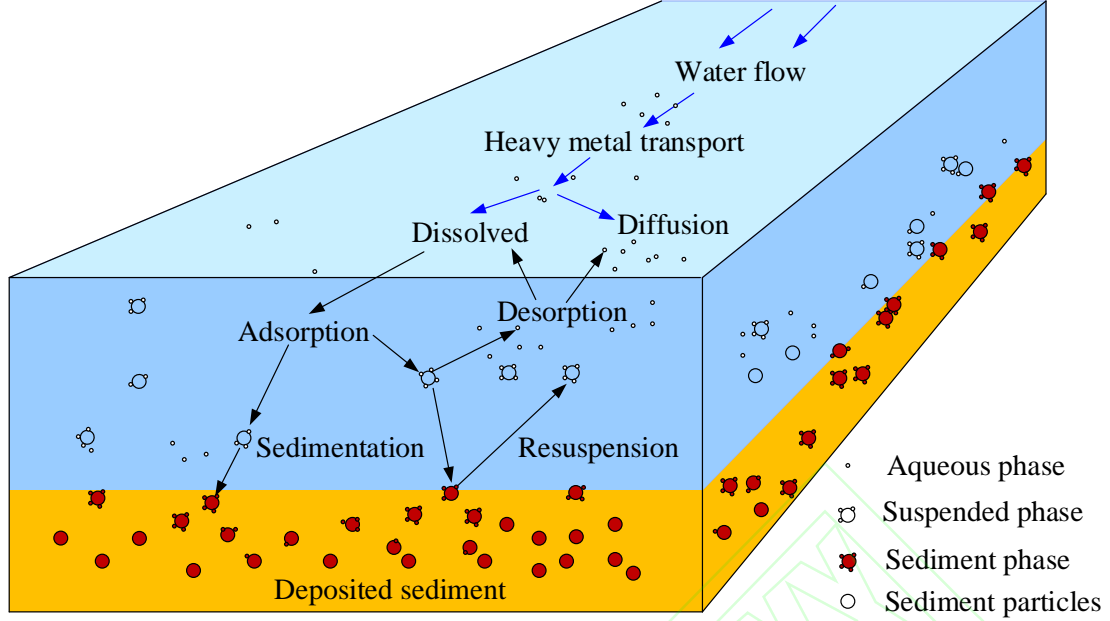
Fig. 2. The transportation and transformation processes of heavy metal in water and sediment

(1) After entering into the water, the heavy metal together with sediment is transferred by water flow. Aone-dimensional hydrodynamic and sediment model was first developed to describe the dynamic process of water and sediment. Then a phase separation model of heavy metal was built for heavy metal migration and transformation simulation. The one-dimensional river hydrodynamics model is based on Saint-Venant equation (Sharafutdinov, 1983). Suspended sediment is the main carrier of heavy metals in water (Lychagin et al., 2017). According to the mass conservation and Newton's second law, the continuous equation of sediment movement and the river bed deformation equations have been established.

Suspended sediment transport equation:

$$\frac{\partial hs_i}{\partial t} + \frac{\partial hus_i}{\partial x} = \frac{\partial}{\partial x}\left(h\varepsilon\frac{\partial s_i}{\partial x}\right) + \omega_{si}\left(S_i^* - s_i\right) \quad (1)$$

River bed distortion equation:

$$\rho_s' \frac{\partial z_{s_i}}{\partial t} = \partial_s \omega_s (s_i - s_{*i}) \quad (2)$$

Sediment carrying capacity:

$$s_{*i} = k[\frac{u^3}{hw}]^m \quad (3)$$

Where, t is time, x is the distance to the start section, u is flow velocity, h is the water depth, z is water elevation, i is the group number of grain diameter, ρ_s' is the

5

density of suspended sediment, S_{*i} is the sediment carrying capacity of water, ω_s is sediment diffusion coefficient, ∂_s is the saturation coefficient of suspended sediment, m is the transport coefficient of suspended sediment.

(2) At the same time, sediment particles affect the storage and transfer status of the heavy metal in water by adsorbing and releasing heavy metals.The chemical properties of heavy metals are stable and not decomposed easily by natural microbes(Ma et al., 2016). After heavy metal pollutants entering into the water, most of the heavy metal will migrate to suspended solids from the water phase due to the adsorption of suspended solids (Herngren et al., 2005). After the load exceeds the carrying capacity of suspension, it will settle down gradually and lead to heavy metal accumulation in the sediment. In some conditions with special temperature and pH, heavy metals can also be decomposed from suspension and sediment and re-enter into the water. The main process of heavy metals'transformation in wateris physical changes, including convection and diffusion with water, adsorption and desorption, settling and resuspension with sediments.The transfer of heavy metals in water is greatly depended on their motion among three phases (Yu and Lu, 2016), which is a process of heavy metal transforming among different phases.The phase separation model of the heavy metal, including the aqueous phase, the suspended phase and the sedimentary phase, has been developed to describe the process (Capone et al., 2004).The phase separation model was developed based on the following assumptions: (1) pH and water temperature are constant, (2) the adsorption process of heavy metal is only related to the sediment conditions, and (3) ignoring the adsorption-desorption process of riverside to heavy metal.

Equations about migration and transformation of heavy metal in the aqueous phase (4), suspended phase (5) and sediment phase (6) are as following:

$$\frac{\partial hc}{\partial t} + \frac{\partial huc}{\partial x} = \frac{\partial}{\partial x}\left(h\varepsilon_w \frac{\partial c}{\partial x} \right) - k_1 \sum_{k=1}^{n_s} h\left(k_b s_k c - c_i \right) + k_4 \left(f_1 - 1 \right)c \quad (4)$$

$$\frac{\partial hc_w}{\partial t} + \frac{\partial huc_w}{\partial x} = \frac{\partial}{\partial x}\left(h\varepsilon_w \frac{\partial c_w}{\partial x} \right) - k_{1s} \sum_{k=1}^{n_s} h\left(k_b s_k c - c_i \right) + \sum_{k=1}^{n_s} \omega_k \alpha_k (S_k^* C_d - S_k C) \quad (5)$$

$$\frac{\partial \eta c_d}{\partial t} = k_1 (c - c_i) - k_4 (f_1 - 1)c - \frac{1}{\rho_\infty} \sum_{k=1}^{n_s} \omega_k \alpha_k (S_k^* C_d - S_k C) \quad (6)$$

Where, c、c_w and c_d are heavy metal concentration in aqueous, suspended and sedimentary sediment phase,respectively; η is the thickness of bottom sediment; ε_w

is turbulent diffusion coefficient; k_1 is the adsorption coefficient; s is the concentration of suspended objects; k_b is the distribution coefficient of suspended material and water; c_i is solution concentration of boundary adsorption; k_4 is desorption coefficient; f_1 is distribution coefficient of sediment phase and water phase; n_s is the total number of groups with different sediment grain diameter; ω_k is total settlement velocity of sediment group number k; S_k^* is sediment carrying capacity of water to sediment group number k; ω is the average settlement velocity of suspended sediment; α is restored saturation coefficient of suspended sediment.

3 CASE STUDIES

3.1 Information about the tailings pond failure accident

As the rainstorm in the upstream of Fujiang River, anelectrolytic *Mn*plant tailings pond failure accident happened on July 27, 2011. The accident threatened the safety ofdrinking water intakes directly in Chongqing city.After the accident, the environmental protection department of Chongqing set 8 sections from the Mixin section (#1), where Fujiang Riverenters into Chongqing city from Sichuan Province, to the intersection between Fujiang River and Jialing River.
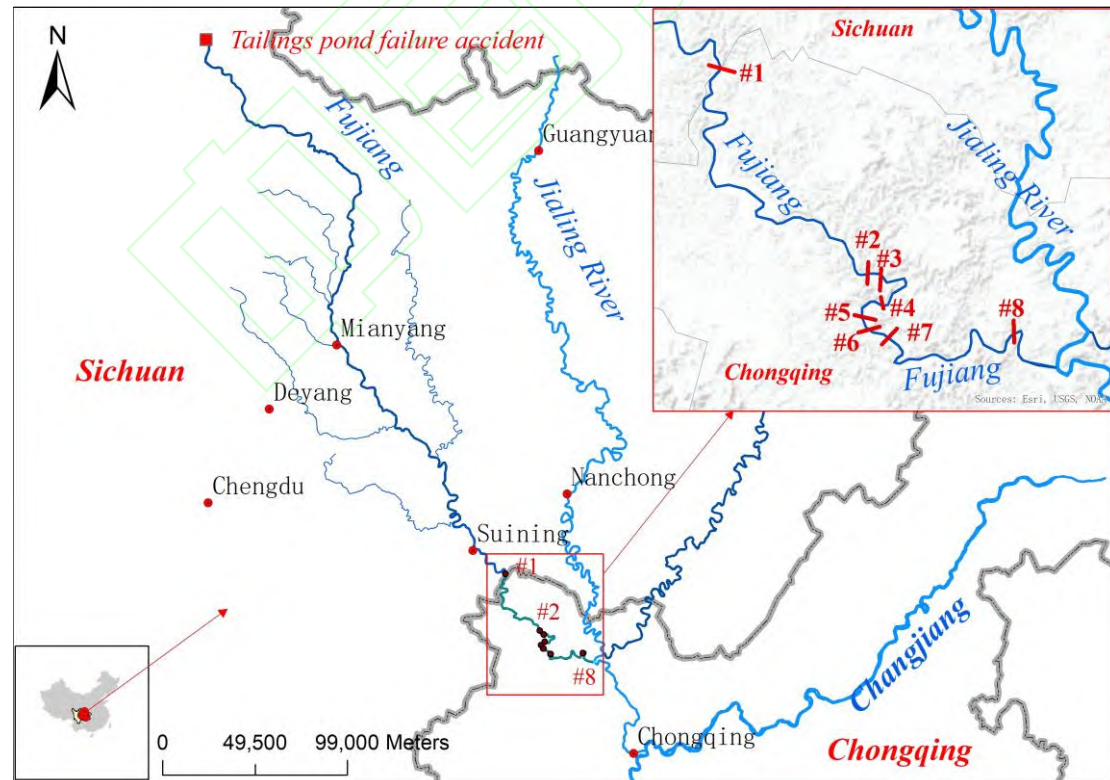

Fig.3. The location of the tailing pond failure accident and the measured data sections

As show in Fig.3, sections #3and #7 are located in drinking water intake areas, which are sensitive and concerned by the government and the masses. This accident was chosen as an example for a case study.

3.2 Model setup

3.2.1 Simulation area and period

The river reaches from section #1 to section #8 (with 108 kilometers length)was treated as simulation area, section #1 was set as inflow headwater.The river reach was divided into 135 one-dimensional computing units with a trapezoid profile. The gradient is set to 0.0005 according to the DEM of this area. Based on the measured concentration changing process of #1 in Fig.4, there is a period that the pollution concentration is over standard (0.1mg/L for drinking water). A simulation was made to answer how pollutants transport in the next three days, from July 29to July 31, 2011.
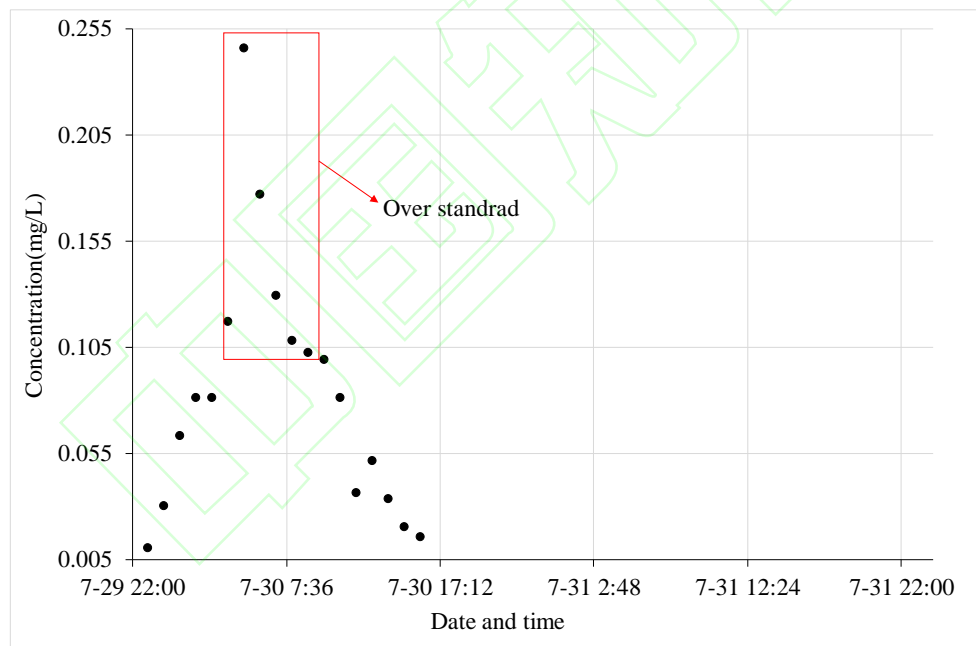

Fig.4. The time series of Mn concentration atsection #1

3.2.2 Initial boundary conditions

Daily hydrological monitoring values (flux at section #1 and water level at section #8) from July 29 to July 31 were treated as boundary conditions. A constant inflow of 500m³/s and concentration changing process of section #1 were set for headwater boundary conditions. The water level was set as 322m for a downstream

boundary. For the sediment model, the average sediment concentration was set as 0.03kg/m^3.

3.3 Model verifications and calibration

Measured data from section #2 and section #4were selected forcalibration. Data in section #6 and section #8 were used for verification. Parameters in different computing elements were set differently. With calibration, values of sensitive parameters were set as shown in table 1.

Table 1 Calibrated parameters of the model

Name	Symbol	Values range
Adsorption coefficient	k_1	$(2.6\sim12.0)\times10^{-12}$
Desorption coefficient	k_4	$(1.6\sim14.0)\times10^{-12}$
Sediment diffusion coefficient	ω_s	$(1.1\sim9.0)\times10^{-10}$
transport coefficient of suspended sediment	m	$(3.5\sim9.0)\times10^{-10}$
The distribution coefficient of sediment phase and water phase	$f1$	$0.01\sim0.04$
The distribution coefficient of suspended material and water phase	k_b	$0.3\sim0.6$

The comparison between simulation results and measured data is shown in Fig.5.
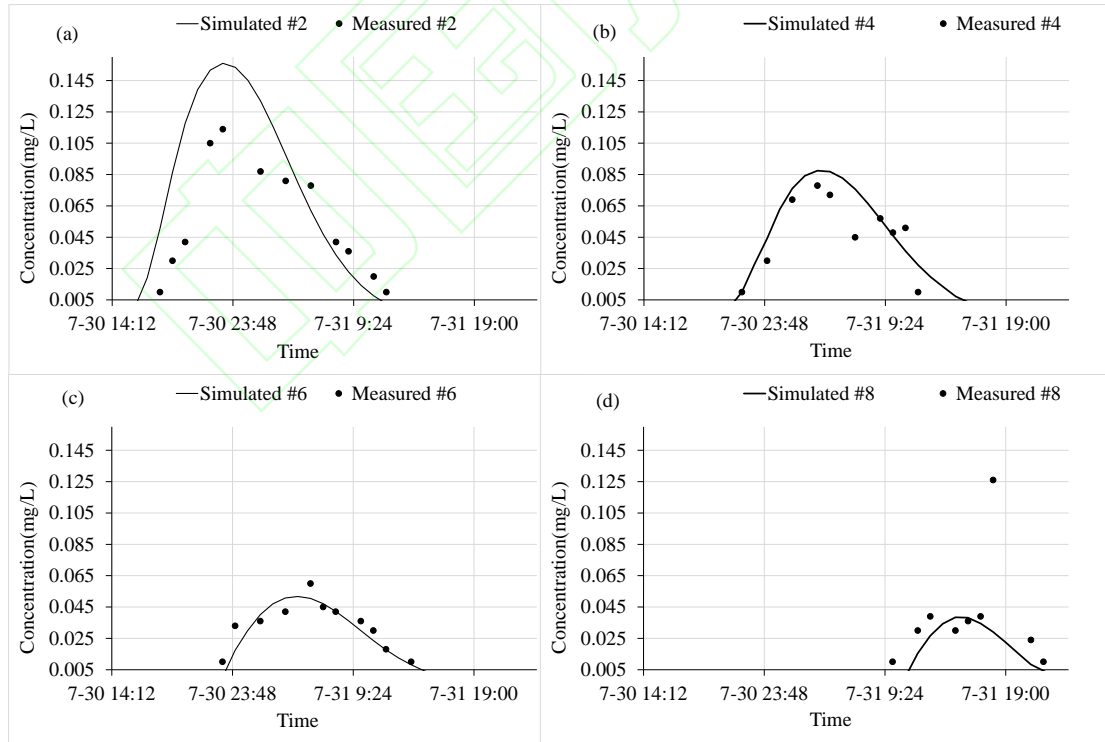

Fig.5. Simulation and measured results of different sections

The comparison between model results and measured data shows that the pollutants moving trends were successfully simulated. There exists a visible

difference between measured and simulated values at #8. At 18:00 July 31, the measured concentration is over 0.125, but the simulated concentration is below 0.045, which caused the average R^2upto0.54 (as shown in Fig.6, (a)). According to the pollutant degradation rule, a monitoring error may be happening.
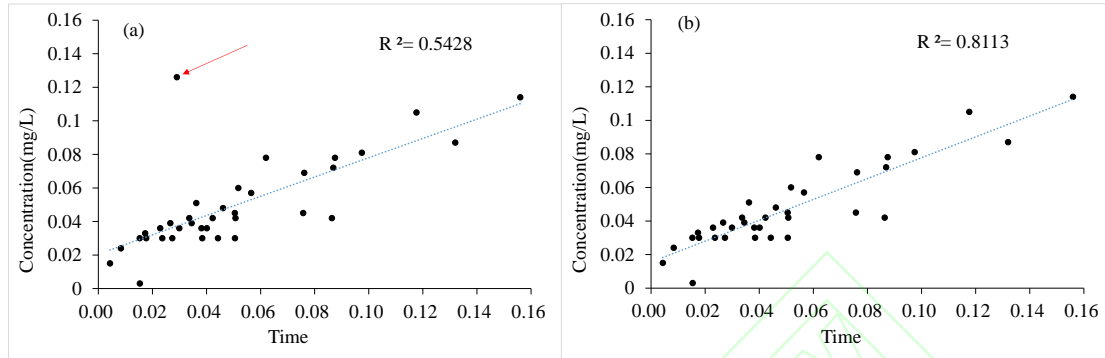

Fig.6. The R^2 between simulated results and measured data. Part (a) contains all measured data, abnormal measured data are deleted in part (b).

Considering the abnormal value, theR^2 is not high enough to prove that the model could accurately predict themigration of Mn. It is also indicated that the model and parameters used in this paper were available for being adopted to simulate the pollutant changing trends after the accident. For a lot of heavy metal models, the R^2ranges from 0.5 to 0.8(Bhuiyan et al., 2016; Kang et al., 2010). With ignoring the abnormal measured value of section #8, the R^2could be 0.81 (Fig.6, (b)). It indicates that the model has good performance for water quality simulation. Due to the lack of measured data of heavy metal in each phase state, the simulation results of heavy metal in each phase state cannot be verified.

3.4 Results and discussion

3.4.1 Changing trends of total concentration in the downstream after the accident

The total concentration of *Mn* in sections #2 to #8 from July 29 to July 31 is shown in Fig.7. The peak concentration value decreased with the increase of distance to #1. The maximum concentration was gradually dropping from 0.156mg/L at #2 (53km away from section #1) to 0.14mg/ L at #3 (71km away from section 1). Lastly, it dropped to 0.038mg/L at 108km away from section #1 at #8.
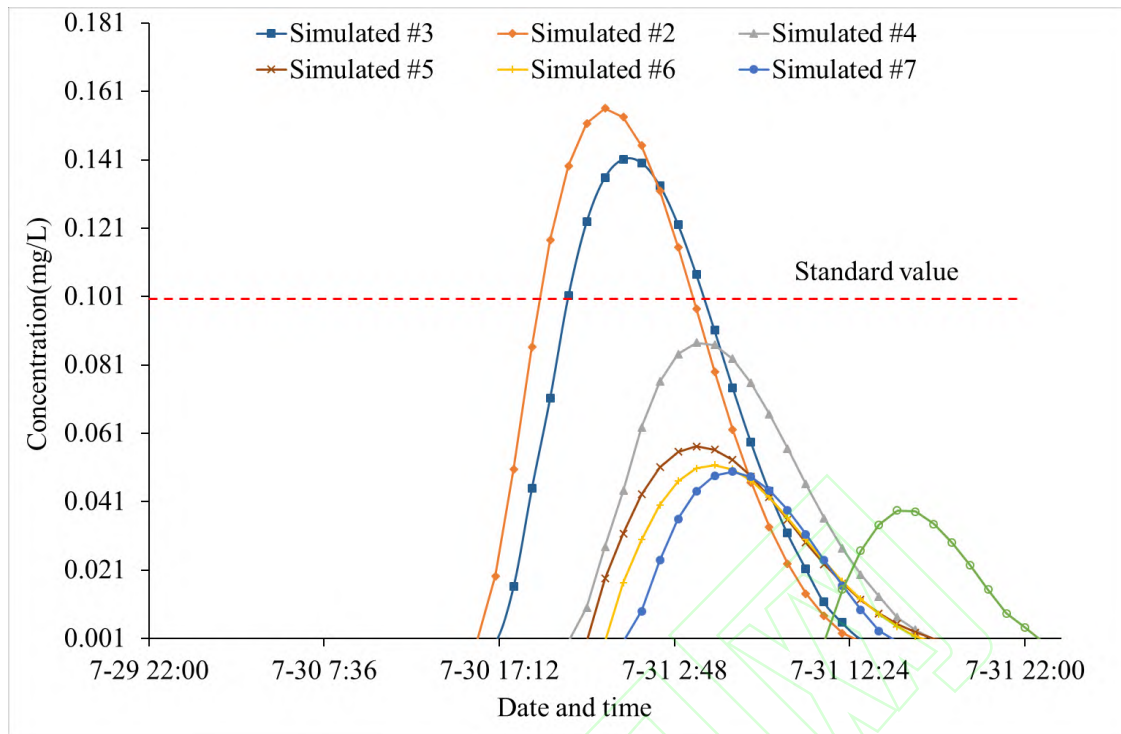
Fig.7. The changing trends of the total concentration of *Mn* in different time

The relationship between the decreasing trend of the maximum concentration of pollutants and distance to #1 is shown in Fig.8.
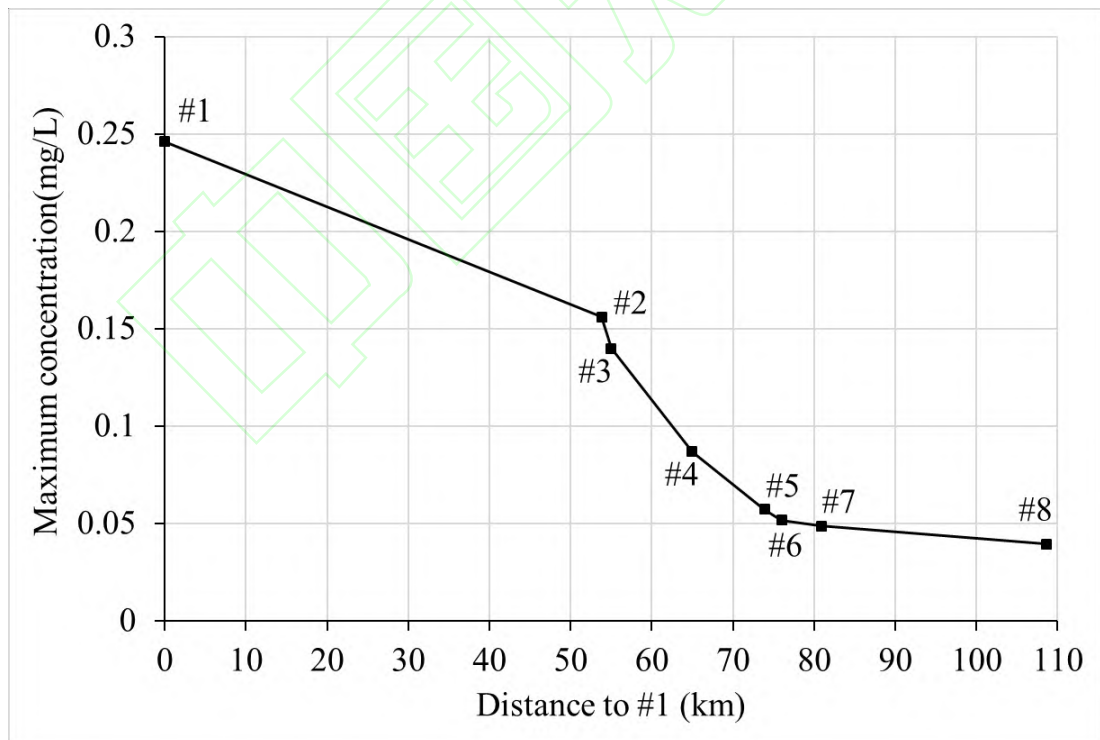

Fig.8. The maximum concentration of Mn in different sections with increasing

distance to section #1

In Fig. 8, it can be seen that the reduction rate of pollutant concentration from

#1to #2is smaller than which from #2 to #6.The rate of peak pollutant reduction decreases from #2 to #8.In particular, from #6 to #8, there is no obvious change on the peak pollutant concentration.At this time, the pollutant concentration is below 0.05mg/L, indicating that the degradation and adsorption of pollutants are less frequent within this concentration range. In the area from section #1 to section #2, the pollutant concentration is relatively high, and the water flow has a greater effect on the transport and diffusion of heavy metals, while the adsorption and desorption effect is relatively small.Due to the action of water flow, the pollutant has a large diffusion, but the concentration reduction rate is relatively low.Atsection #2, the pollutant concentration drops to 0.15mg/L. In this situation, with concentration decreasing and flow velocity slowing down, the effect of water flow on heavy metal transport and diffusion becomes smaller, and the effect of adsorption and desorption increases relatively(Qian et al., 2014; Undabeytia et al., 2005).It indicates that, when the pollutant concentration is high, the diffusion effect has a great influence on the concentration change of heavy metals(Huang et al., 2015). When the concentration is reduced to a certain extent, adsorption and desorption play a major role in the pollutant concentration changing(Shi et al., 2013).With a further decrease of the concentration, the adsorption, desorption and diffusion are relatively weakened, and the concentration remains stableat some extent.In this accident, when the concentration of *Mn* is around 0.05, the diffusion, adsorption and desorption maintain a slow speed.

3.4.2 Duration time and areas of concentration over standard

For the regional section #1 to section #8, the duration time of pollutant concentration over standard is shown in Fig.9.
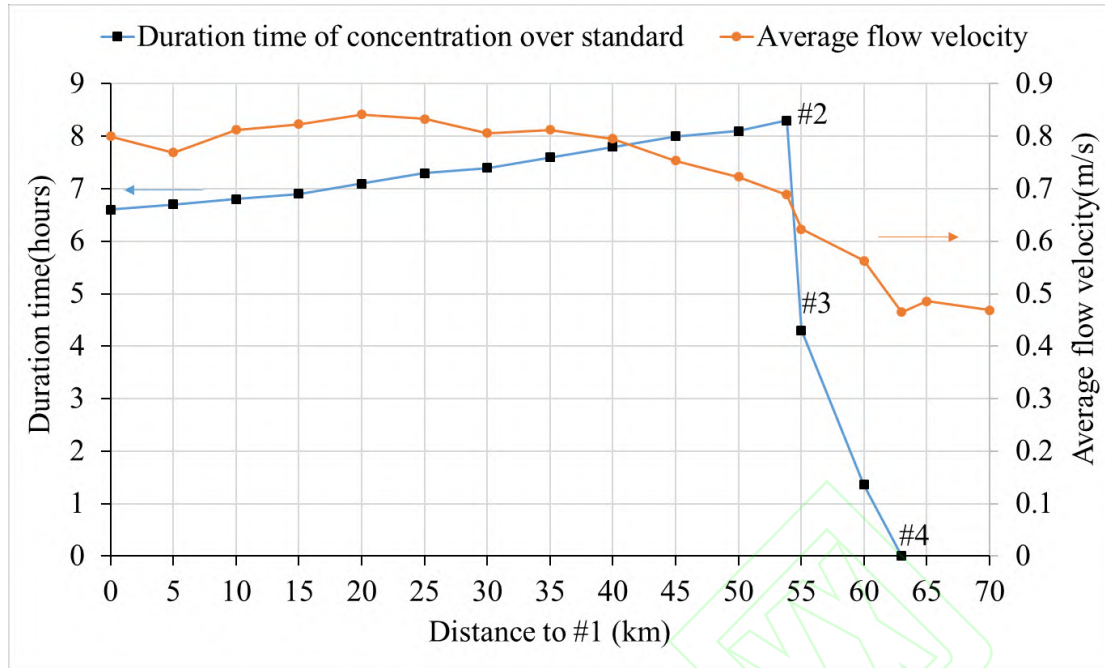
Fig.9. Duration time of concentration over standard and average flow velocity at different sections with the distance to #1 increasing

Combined with Fig.7 and Fig.9, it can be noticed that the tailing pond failure accident caused the pollutant concentration exceeding the standard in the river to reach 62km distance away from #1. The duration time of concentration over standard showed an upward trend from #1 to 53km downstream. This sudden accident caused the pollutant concentration to exceed the standard in section #2 and section #3. The pollutant concentration in section #2 began to rise at 17:00 on July 30. At 19:30, it was close to exceed the standard and continued to rise until 23:00, when the concentration reached the maximum value of 0.156. After that, the pollutant concentration decreased and then dropped to the standard value at about 3:50 on July 31.It was indicated that the pollutant concentration in section# 2 exceeded the standard causing by the accident, lasting for 8 hours and 20 minutes.The same trend also happened in the section# 2 and #3. The over standard time started from 21:00 on July 30 and ended until 4:20 on July 31 at #3, lasting for 7 hours and 20 minutes. As there is a drinking water source area at section #3, it is indispensable to make early warning and alert to ensure the drinking water safety.Section #7 is also the source of drinking water, but the maximum concentration of pollutants at this location is 0.05mg/L, which is below the standard value. Thus, the water can be taken normally as usual in section #7. The reaches where manganese concentration over standard was shown in Fig.10.
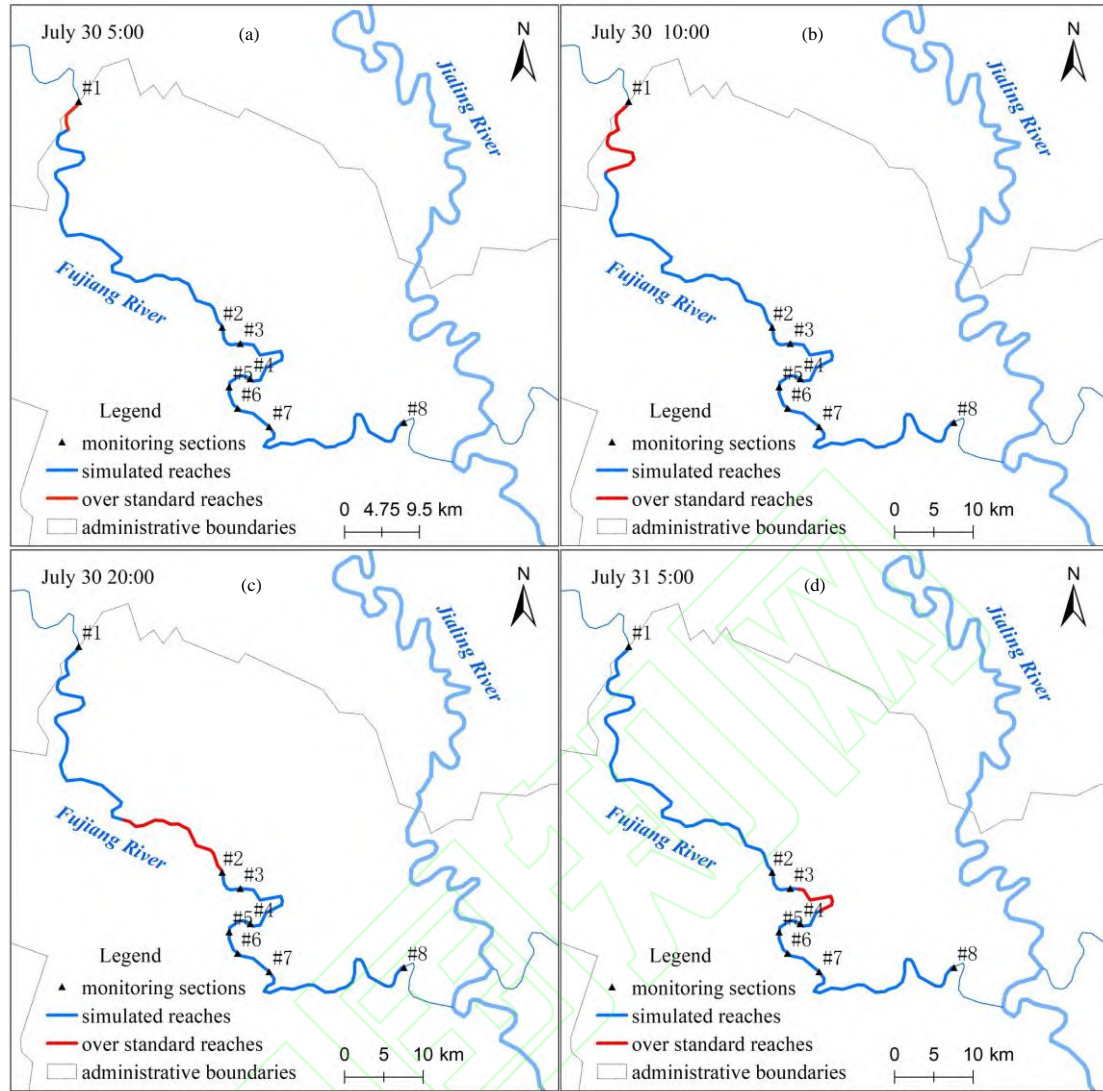
Fig.10. The river reaches where *Mn* concentration over standard transport process after tailings pondfailure accident

As shown in Fig.10, due to the flow velocity decreases, the diffusion of pollutants slows down. The length of reaches over standard in the upstream of section #2 is longer than the downstream of #2. For example, at 20:00 on July 30, the length of over standard reaches is 16.3 kilometers,which is double than the length of over standard reaches at 5:00 on July 31. From the morphology view of polluted reaches, the area of manganese concentration over standard reaches expands in the higher concentration and then contracts in the smaller concentration.The variation process of the duration time for the heavy metal pollution concentration is related to pollutant concentration and flow velocity(Thakur et al., 2019). The water flow movement increases the pollutant diffusion and polluted area, but decreases pollutant

degradation(Kaserzon et al., 2014), which leads to a longer duration time of pollutant concentration over standard.

3.4.3 Pollutants concentration distribution of different phrases

For water quality accident early warning, the previous studies focus on soluble substance, most of them only point out the total concentration of pollutants(Hasan et al., 2005; Wang et al., 2015). For much pollutions, sediment adsorption has a great influence on the contamination situation. A large number of studies have shown that heavy metals are not easily decomposed by microorganisms and are difficult to produce biochemical and chemical reactions. Most of the heavy metal are adsorbed into the sediments and some of them sink into the river bottom mud (Bhatnagar et al., 2011). However, these adsorption and desorption processes have been ignored by the previous studies for water quality accident early warning(Huan et al., 2020; Wang et al., 2018). In contrast,with the sediment model and phase model, the impact of sediments has been considered and the concentration of different phases in this study has been obtained, as shown in Fig.11.
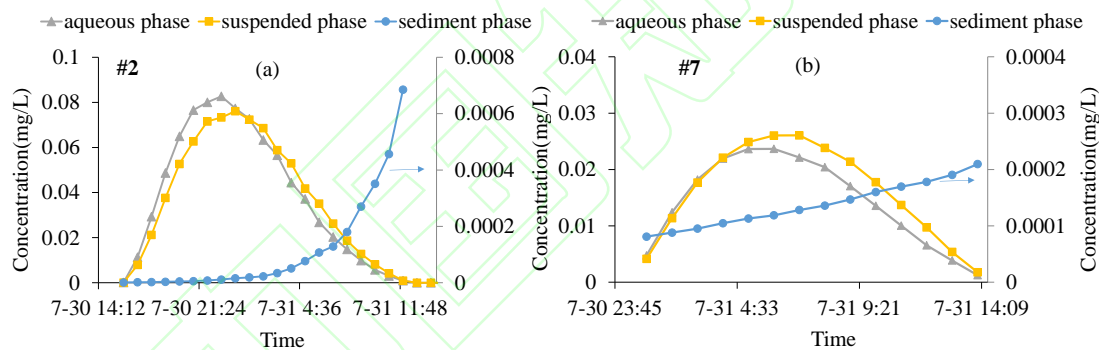

Fig. 11. Manganeseconcentration of different phases at section #2 and section #7

From July 20 14:00 to July 31 11:48, the concentration of heavy metal in the bottom sediment phase increases continuously at section #2. The Manganese concentration of the aqueous phase is higher than which of the suspended phase before July 31 1:00 at section #2. But after that, the concentration of the suspended phase becomeshigher. There are similar changing trends of bottom sediment phase at section #7. It is indicated that the adsorption function is greater than the desorption functionas time goes on.By comparing the concentration of different phases at section #2 and section #7 together with flow velocity variation trend, it is demonstrated that the sedimentation and resuspension of sediment are enhanced with the decrease of water velocity from the upstream to the downstream of the river(Kaserzon et al., 2014). After July 31 1:00 at section #2 and 4:30 at section #7, the *Mn*is gradually

adsorbed by suspended sediments and deposited, which leads to the increase of heavy metal concentration in the suspended and sediment phase. Meanwhile, the adsorption rate and adsorption amount of sediment are inversely proportional to their particle size(Buyang et al., 2019). As the particle size of the bed sediment mass is larger than that of the suspended mass, the adsorption rate of the suspended mass of the aqueous phase, heavy metal is greater than that of the bed sediment mass.This leads to the phenomenon that the *Mn* concentration of the suspended phase is always larger than the *Mn* concentration of the sediment phase in two sections.

Overall, the water flow slows down due to the widening of the water surface area in section #2.According to the theory of sediment kinematics, there is an inversely proportional relationship between the sedimentation velocity of sediment and flow velocity(Kozerski, 2002). Along with the flow rate slowing down, the adsorption rate of pollutants increases. Itcausesa large number of the heavy metal sink to the bottom of the water. As a result, the concentration of pollutants decreases at a higher rate, and the duration time of pollutants over standard could be reduced. With further pollutant adsorption and sedimentation, the duration time of pollutants exceeding the standard was dropped down to 0 at 63km. It is indicated that most of the heavy metal in the water was absorbed by sediment mass.

4 CONCLUSION

Based on the transfer and transformation mechanism of heavy metal, a phase model of heavy metal migration and transformation was established by considering the influence of sediment on the heavy metal. It has been applied to simulate the impact of sudden accidents on the downstream of tailings ponds.The verification results showed that the model exhibited good performance in rapidly simulating the variation trend of the heavy metal *Mn*. By setting the measured data in the upstream as conditions, the pollutant concentration in the downstream and early warning have been simulated after a tailing pond failure accident. Results showed that the accident would lead to a concentration of 63km reaches in Fujiang River exceeding the standard in Chongqing City. A drinking water source near section #3 will be polluted and last for 7 hours. Additionally, the results also indicate that the migration of heavy metal pollutants is mainly affected by water transport. But the decrease of heavy metal concentration is mainly affected by sediment adsorption.There is a negative

correlation between the pollutant concentration reduction rate and *Mn* concentration and flow velocity.The adsorption and settlement rate will increase if the flow velocity decreases and the *Mn* concentration is less than 0.15mg/L, which is conducive to the reduction of *Mn* concentration.Heavy metal pollution after tailing pond failure accident was better simulated in this paper, which is an application extension in the field of water quality accident early warning.It can provide support for accident disposal and early warning through simulating water quality concentration change processes in the downstream based on the measurement data of the upstream.

CONFLICTS OF INTEREST

The authors have no conflicts of interest to declare.

ACKNOWLEDGEMENTS

REFERENCES CITED

Agurto-Detzel, H., Bianchi, M., Assump ção, M., Schimmel, M., Colla ço, B., Ciardelli, C., Barbosa, J.R., Calhau, J., 2016. The tailings dam failure of 5 November 2015 in SE Brazil and its preceding seismic sequence. Geophys. Res. Lett. 43, 4929–4936. https://doi.org/10.1002/2016GL069257

Ani, E.C., Cristea, V.M., Agachi, P.S., 2012. Mathematical models to support pollution counteraction in case of accidents. Environ. Eng. Manag. J. 11, 13–20. https://doi.org/10.30638/eemj.2012.003

Bambach, M., Heinkenschloss, M., Herty, M., 2013. A method for model identification and parameter estimation. Inverse Probl. 29. https://doi.org/10.1088/0266-5611/29/2/025009

Bhatnagar, A., Vilar, V.J.P., Botelho, C.M.S., Boaventura, R.A.R., 2011. A review of the use of red mud as adsorbent for the removal of toxic pollutants from water

and wastewater. Environ. Technol. 32, 231–249. https://doi.org/10.1080/09593330.2011.560615

Bhuiyan, M.A.H., Bodrud-Doza, M., Islam, A.R.M.T., Rakib, M.A., Rahman, M.S., Ramanathan, A.L., 2016. Assessment of groundwater quality of Lakshimpur district of Bangladesh using water quality indices, geostatistical methods, and multivariate analysis. Environ. Earth Sci. 75. https://doi.org/10.1007/s12665-016-5823-y

Buyang, S., Yi, Q., Cui, H., Wan, K., Zhang, S., 2019. Distribution and adsorption of metalson different particle size fractions of sediments in a hydrodynamically disturbed canal. Sci. Total Environ. 670, 654–661. https://doi.org/10.1016/j.scitotenv.2019.03.276

Capone, M., Sangiovanni, G., Castellani, C., Di Castro, C., Grilli, M., 2004. Phase Separation Close to the Density-Driven Mott Transition in the Hubbard-Holstein Model. Phys. Rev. Lett. 92. https://doi.org/10.1103/PhysRevLett.92.106401

Chen, S., Wu, C., Yang, F.Q., Bao, R.X., 2011. Heavy metal pollution model of tailings and the pollution simulation by visualization. J. Coal Sci. Eng. 17, 355–359. https://doi.org/10.1007/s12404-011-0325-8

Chen, Y., Xu, S., Jin, Y., 2016. Evaluation on ecological restoration capability of revetment in inland restricted channel. KSCE J. Civ. Eng. 20, 2548–2558. https://doi.org/10.1007/s12205-015-0291-6

Criss, R.E., Yao, W., Li, C., Tang, H., 2020. A Predictive, Two-Parameter Model for the Movement of ReservoirLandslides. J. Earth Sci. https://doi.org/10.1007/s12583-020-1331-9

Dalali, N., Habibi, H., 2015. Facilitated transport of cadmium by bulk liquid membrane using Aliquat 336 as carrier: separation from other heavy metal ions. Desalin. Water Treat. 56, 1601–1609. https://doi.org/10.1080/19443994.2014.951973

Ding, X., Zhang, J., Jiang, G., Zhang, S., 2017. Early warning and forecasting system of water quality safety for drinking water source areas in Three Gorges Reservoir Area, China. Water (Switzerland) 9. https://doi.org/10.3390/w9070465

Djihouessi, M.B., Aina, M.P., 2018. A review of hydrodynamics and water quality of Lake Nokoué: Current state of knowledge and prospects for further research. Reg. Stud. Mar. Sci. 18, 57–67. https://doi.org/10.1016/j.rsma.2018.01.002

Grayman, W.M., Deninger, R.A., Males, R., 2001. Design of Early Warning and Predictive Source-Water Monitoring Systems 328.

Hasan, J., Goldbloom-Helzner, D., Ichida, A., Rouse, T., Gibson, M., 2005. Technologies and Techniques for Early Warning Systems to Monitor and Evaluate Drinking Water Quality : A State-of-the-Art Review. EPA United States Enviromental Prot. Agency 165.

Helios Rybicka, E., Calmano, W., Breeger, A., 1995. Heavy metals sorption/desorption on competing clay minerals; an experimental study. Appl. Clay Sci. 9, 369–381. https://doi.org/10.1016/0169-1317(94)00030-T

Herngren, L., Goonetilleke, A., Ayoko, G.A., 2005. Understanding heavy metal and suspended solids relationships in urban stormwater using simulated rainfall. J. Environ. Manage. 76, 149–158. https://doi.org/10.1016/j.jenvman.2005.01.013

Huan, H., Li, X., Zhou, J., Liu, W., Li, J., Liu, B., Xi, B., Jiang, Y., 2020. Groundwater pollution early warning based on QTR model for regional risk management: A case study in Luoyang city, China. Environ. Pollut. 259. https://doi.org/10.1016/j.envpol.2019.113900

Huang, Q., Cai, X., Alhadj Mallah, M.M., Chi, Y., Yan, J., 2015. Effect of HCl/SO2/NH3/O2 and mineral sorbents on the partitioning behaviour of heavy metals during the thermal treatment of solid wastes. Environ. Technol. (United Kingdom) 36, 3043–3049. https://doi.org/10.1080/09593330.2014.963693

Jacobson, R., Faust, T., 2014. Hydrologic connectivity of floodplains, northern missouri-implications for management and restoration of floodplain forest communities in disturbed landscapes. River Res. Appl. 30, 269–286. https://doi.org/10.1002/rra.2636

Jähnig, S.C., Cai, Q., 2010. River water quality assessment in selected Yangtze tributaries: Background and method development. J. Earth Sci. 21, 876–881. https://doi.org/10.1007/s12583-010-0140-y

Kang, J.H., Lee, S.W., Cho, K.H., Ki, S.J., Cha, S.M., Kim, J.H., 2010. Linking land-use type and stream water quality using spatial data of fecal indicator bacteria and heavy metals in the Yeongsan river basin. Water Res. 44, 4143–4157. https://doi.org/10.1016/j.watres.2010.05.009

Kaserzon, S.L., Hawker, D.W., Booij, K., O'Brien, D.S., Kennedy, K., Vermeirssen, E.L.M., Mueller, J.F., 2014. Passive sampling of perfluorinated chemicals in water: In-situ calibration. Environ. Pollut. 186, 98–103. https://doi.org/10.1016/j.envpol.2013.11.030

Kozerski, H.P., 2002. Determination of areal sedimentation rates in rivers by using plate sediment trap measurements and flow velocity - Settling flux relationship. Water Res. 36, 2983–2990. https://doi.org/10.1016/S0043-1354(01)00533-4

Lychagin, M., Chalov, S., Kasimov, N., Shinkareva, G., Jarsjö, J., Thorslund, J., 2017. Surface water pathways and fluxes of metals under changing environmental conditions and human interventions in the Selenga River system. Environ. Earth Sci. 76. https://doi.org/10.1007/s12665-016-6304-z

Ma, L., Wang, Q., Islam, S.M., Liu, Y., Ma, S., Kanatzidis, M.G., 2016. Highly Selective and Efficient Removal of Heavy Metals by Layered Double Hydroxide Intercalated with the MoS42- Ion. J. Am. Chem. Soc. 138, 2858–2866. https://doi.org/10.1021/jacs.6b00110

Qian, L., Ma, M., Cheng, D., 2014. The effect of water chemistry on adsorption and desorption of U(VI) on nano-alumina. J. Mol. Liq. 197, 295–300. https://doi.org/10.1016/j.molliq.2014.05.026

Rafiei, B., Ghomi, F.A., Ardebili, L., Sadeghifar, M., Sharifi, S.H.K., 2012. Distribution of Metals (Cu, Zn, Pb, and Cd) in Sediments of the Anzali Lagoon, North Iran. Soil Sediment Contam. 21, 768–787. https://doi.org/10.1080/15320383.2012.678953

Sadeghi, S.H.R., Kiani Harchegani, M., Younesi, H.A., 2012. Suspended sediment concentration and particle size distribution, and their relationship with heavy metal content. J. Earth Syst. Sci. 121, 63–71. https://doi.org/10.1007/s12040-012-0143-4

Shah, B.A., Shah, A. V., Mistry, C.B., Navik, A.J., 2013. Assessment of heavy metals in sediments near Hazira industrial zone at Tapti River estuary, Surat, India. Environ. Earth Sci. 69, 2365–2376. https://doi.org/10.1007/s12665-012-2066-4

Sharafutdinov, V.A., 1983. A problem of integral geometry for tensor fields and the St. Venant equation. Sib. Math. J. 24, 968–977. https://doi.org/10.1007/BF00970323

Shi, Z., Di Toro, D.M., Allen, H.E., Sparks, D.L., 2013. A general model for kinetics of heavy metal adsorption and desorption on soils. Environ. Sci. Technol. 47, 3761–3767. https://doi.org/10.1021/es304524p

Storey, M. V., van der Gaag, B., Burns, B.P., 2011. Advances in on-line drinking water quality monitoring and early warning systems. Water Res. 45, 741–747. https://doi.org/10.1016/j.watres.2010.08.049

Thakur, C.K., Chaudhary, M., Van Der Zee, S.E.A.T.M., Singh, M.K., 2019. Two-dimensional solute transport with exponential initial concentration distribution and varying flow velocity. Pollution 5, 721–737. https://doi.org/10.22059/poll.2019.275005.574

Undabeytia, T., Nir, S., Rytwo, G., Serban, C., Morillo, E., Maqueda, C., 2005. Modeling adsorption-desorption processes of Cu on montmorillonite and the effect of competitive adsorption with a cationic pesticide. React. Transp. Soil Groundw. Process. Model. 79–91. https://doi.org/10.1007/3-540-26746-8_6

Wang, Y., Engel, B.A., Huang, P., Peng, H., Zhang, X., Cheng, M., Zhang, W., 2018. Accurately early warning to water quality pollutant risk by mobile model system with optimization technology. J. Environ. Manage. 208, 122–133. https://doi.org/10.1016/j.jenvman.2017.12.006

Wang, Y., Liu, R. hai, Zhang, Y. qing, Cui, X. qing, Tang, A. kun, Zhang, L. jun, 2016. Transport of heavy metals in the Huanghe River estuary, China. Environ. Earth Sci. 75, 1–11. https://doi.org/10.1007/s12665-015-4908-3

Wang, Y., Zhang, W., Engel, B.A., Peng, H., Theller, L., Shi, Y., Hu, S., 2015. A fast mobile early warning system for water quality emergency risk in ungauged river basins. Environ. Model. Softw. 73, 76–89.

https://doi.org/10.1016/j.envsoft.2015.08.003

Winner, R.W., Boesel, M.W., Farrell, M.P., 1980. Insect community structure as an index of heavy metal pollution in lotic ecosystems. Can. J. Fish. Aquat. Sci. 37, 647–655. https://doi.org/10.1139/f80-081

Yu, G., Song, C., Pan, Y., Li, L., Li, R., Lu, S., 2014. Review of new progress in tailing dam safety in foreign research and current state with development trent in China. Yanshilixue Yu Gongcheng Xuebao/Chinese J. Rock Mech. Eng. 33, 3238–3248.

Yu, X., Lu, S., 2016. Multiscale correlations of iron phases and heavy metals in technogenic magnetic particles from contaminated soils. Environ. Pollut. 219, 19–27. https://doi.org/10.1016/j.envpol.2016.09.053

Yuanhua, C., Jiping, J., Yu, L., Lina, Z., Yi, W., 2013. A GIS-based early warning and emergency decision support system for river heavy metal pollution incidents. Adv. Mater. Res. 664, 399–402. https://doi.org/10.4028/www.scientific.net/AMR.664.399